# REPORT DOCUMENTATION PAGE

Form Approved OMB NO. 0704-0188



| 1. REPORT DATE (DD-MM-YYYY) | 2. REPORT TYPE | 3. DATES COVERED (From - To) |
|---|---|---|
| 03-04-2011 | Final Report | 29-Sep-2010 - 27-Mar-2011 |

4. TITLE AND SUBTITLE

1.5 Micron Photonic Devices Based on III-nitrides Grown on Si Substrates

5a. CONTRACT NUMBER

5b. GRANT NUMBER

W911NF-10-C-0073

5c. PROGRAM ELEMENT NUMBER

665502

6. AUTHORS

Jing Li

5d. PROJECT NUMBER

5e. TASK NUMBER

5f. WORK UNIT NUMBER

7. PERFORMING ORGANIZATION NAMES AND ADDRESSES

III-N Technology, Inc.
4627 5th Street

Lubbock, TX 79416 -4727

8. PERFORMING ORGANIZATION REPORT NUMBER

9. SPONSORING/MONITORING AGENCY NAME(S) AND ADDRESS(ES)

U.S. Army Research Office
P.O. Box 12211
Research Triangle Park, NC 27709-2211

10. SPONSOR/MONITOR'S ACRONYM(S)

ARO

11. SPONSOR/MONITOR'S REPORT NUMBER(S)

58718-EL-ST1.1

12. DISTRIBUTION AVAILIBILITY STATEMENT

Approved for Public Release; Distribution Unlimited

13. SUPPLEMENTARY NOTES

The views, opinions and/or findings contained in this report are those of the author(s) and should not contrued as an official Department of the Army position, policy or decision, unless so designated by other documentation.

14. ABSTRACT

Report developed under topic #A10AT015, contract W911NF-10-C-0073. Our goal is to provide the technology base for realizing monolithic emitters and optical amplifiers active at 1.5 micron on Si substrates that are compatible with standard processes of the complementary metal-oxide-semiconductor (CMOS) technology. Our approach is to exploit epitaxial growth of III-nitride semiconductors on Si substrate and in-situ erbium (Er) doping of III-nitrides. During the Phase I supporting period, 3N has demonstrated proof-of-concept of a technology for

15. SUBJECT TERMS

STTR Report

| 16. SECURITY CLASSIFICATION OF: | | | 17. LIMITATION OF ABSTRACT | 15. NUMBER OF PAGES | 19a. NAME OF RESPONSIBLE PERSON |
|---|---|---|---|---|---|
| a. REPORT | b. ABSTRACT | c. THIS PAGE | | | Jing Li |
| UU | UU | UU | UU | | 19b. TELEPHONE NUMBER: 806-401-9289 |

**Report Title**

1.5 Micron Photonic Devices Based on III-nitrides Grown on Si Substrates


**ABSTRACT**

Report developed under topic #A10AT015, contract W911NF-10-C-0073. Our goal is to provide the technology base for realizing monolithic emitters and optical amplifiers active at 1.5 micron on Si substrates that are compatible with standard processes of the complementary metal-oxide-semiconductor (CMOS) technology. Our approach is to exploit epitaxial growth of III-nitride semiconductors on Si substrate and in-situ erbium (Er) doping of III-nitrides. During the Phase I supporting period, 3N has demonstrated proof-of-concept of a technology for growth of Er doped III-nitride photonic device structures on (001) Si substrates. More specifically, InGaN:Er and GaN:Er films and p-i-n junction (p-GaN/InGaN/n-GaN:Er) devices operating at 1.54 um wavelength have been designed, fabricated and characterized. Our Phase I results have demonstrated the feasibility to develop active photonic devices operating at wavelength around 1.54 um on silicon wafers that are CMOS compatible.


## List of papers submitted or published that acknowledge ARO support during this reporting period. List the papers, including journal references, in the following categories:

### (a) Papers published in peer-reviewed journals (N/A for none)

**Number of Papers published in peer-reviewed journals:** 0.00

### (b) Papers published in non-peer-reviewed journals or in conference proceedings (N/A for none)

**Number of Papers published in non peer-reviewed journals:** 0.00

### (c) Presentations

**Number of Presentations:** 0.00

### Non Peer-Reviewed Conference Proceeding publications (other than abstracts):

**Number of Non Peer-Reviewed Conference Proceeding publications (other than abstracts):** 0

### Peer-Reviewed Conference Proceeding publications (other than abstracts):

**Number of Peer-Reviewed Conference Proceeding publications (other than abstracts):** 0

### (d) Manuscripts

**Number of Manuscripts:** 0.00

### Patents Submitted

### Patents Awarded

## Awards

### Graduate Students

| NAME | PERCENT_SUPPORTED |
|---|---|
| I-Wen Feng | 0.50 |
| **FTE Equivalent:** | **0.50** |
| **Total Number:** | **1** |

### Names of Post Doctorates

| NAME | PERCENT_SUPPORTED |
|---|---|
| **FTE Equivalent:** | |
| **Total Number:** | |

### Names of Faculty Supported

| NAME | PERCENT_SUPPORTED |
|---|---|
| **FTE Equivalent:** | |
| **Total Number:** | |

### Names of Under Graduate students supported

| NAME | PERCENT_SUPPORTED |
|---|---|
| **FTE Equivalent:** | |
| **Total Number:** | |

### Student Metrics

This section only applies to graduating undergraduates supported by this agreement in this reporting period

| | |
|---|---|
| The number of undergraduates funded by this agreement who graduated during this period: ..... | 0.00 |
| The number of undergraduates funded by this agreement who graduated during this period with a degree in science, mathematics, engineering, or technology fields:..... | 0.00 |
| The number of undergraduates funded by your agreement who graduated during this period and will continue to pursue a graduate or Ph.D. degree in science, mathematics, engineering, or technology fields:..... | 0.00 |
| Number of graduating undergraduates who achieved a 3.5 GPA to 4.0 (4.0 max scale): ..... | 0.00 |
| Number of graduating undergraduates funded by a DoD funded Center of Excellence grant for Education, Research and Engineering: ..... | 0.00 |
| The number of undergraduates funded by your agreement who graduated during this period and intend to work for the Department of Defense ..... | 0.00 |
| The number of undergraduates funded by your agreement who graduated during this period and will receive scholarships or fellowships for further studies in science, mathematics, engineering or technology fields: ..... | 0.00 |

### Names of Personnel receiving masters degrees

| NAME |
|---|
| **Total Number:** |

## Names of personnel receiving PHDs

| NAME |
| --- |
| **Total Number:** |

## Names of other research staff

| NAME | PERCENT SUPPORTED |
| --- | --- |
| **FTE Equivalent:** | |
| **Total Number:** | |

## Sub Contractors (DD882)

## Inventions (DD882)

## Scientific Progress

See attached

## Technology Transfer

III-N Technology, Inc
1.5 µm Photonic Devices Based on III-nitrides Grown on Si Substrates
ARMY STTR A10a-T015: Photonic Amplifiers Based on III-nitrides Grown on Si Substrates

# Final Technical Report

The name of the contractor: III-N Technology, Inc.
The contract number: W911NF-10-C-0073
The Contract Line Item Number (CLIN) being billed against: 0002 (Sub-CLIN: 0002AF)
The period of performance: 09/30/2010 – 03/31/2011

## A. Introduction

During the Phase I supporting period, 3N has demonstrated proof-of-concept of a technology for growth of Er doped III-nitride photonic device structures on (001) Si substrates. More specifically, InGaN:Er and GaN:Er films and p-i-n junction (p-GaN/InGaN/n-GaN:Er) devices operating at 1.54 µm wavelength have been designed, fabricated and characterized. Our Phase I results have demonstrated the feasibility to develop active photonic devices operating at wavelength around 1.54 µm on silicon wafers that are CMOS compatible. We believe this demonstration is significant because the technology once fully developed is expected to lead to monolithic photonic integrated circuits (PIC) on Si. Such PIC devices can address the growing limitations facing chip-scale data transport and will be an important step towards all-optical integrated circuits, accelerating the convergence of computing and telecommunications. The technology will also have widespread military applications including optical communication networks, IR countermeasures, optical signal processing, and free space communications. We have submitted Phase II proposal for STTR topic A10a-T015 and the results of the phase I work were summarized in the Phase II full proposal:

## B. Results of the Phase I Work

### B1. Growth and conductivity controlling of Er doped InGaN alloys

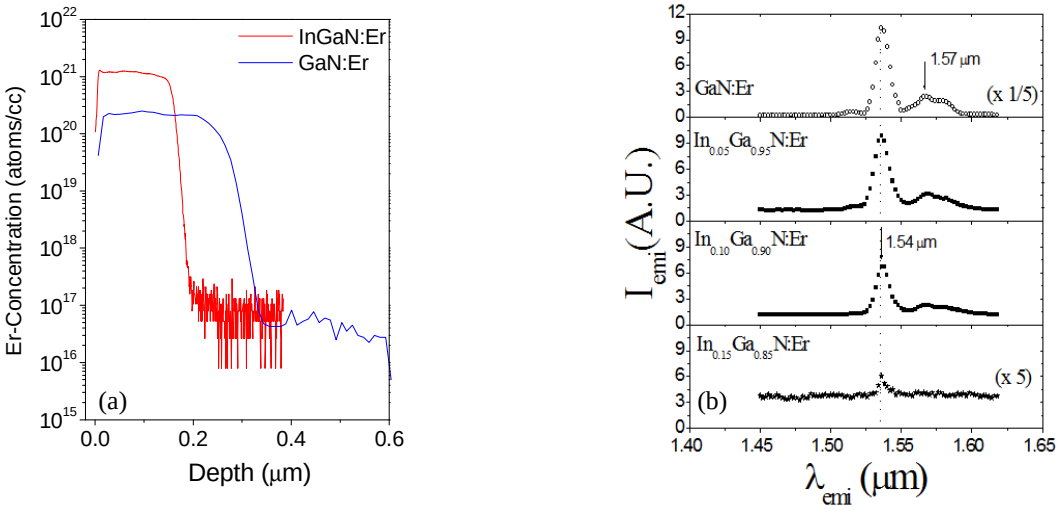


Figure 1 (a) SIMS profiles of Er concentrations in GaN and InGaN. (b) PL spectra of GaN:Er and InGaN:Er in 1.54 µm region.

One of the objectives of this project is to achieved Er doped InGaN to allow bandgap engineering via InGaN/GaN heterostructures to enhance the efficiency of 1.54 µm emitters. The growth of Er-doped InGaN epilayers with an efficient 1.54 µm emission has been challenging. This

is because the optimal growth temperatures for the incorporation of Er ions on optically active sites and for InGaN are not compatible. For instance, the optimal growth temperature for the incorporation of Er ions in III-nitrides is generally ~1000 $^{o}$C, while the epi-growth temperature of InGaN epilayers is much lower (near or below 760 $^{o}$C). We have carried out preliminary studies on growth of Er doped $In_xGa_{1-x}N$ (InGaN:Er) epilayers on various templates. Our results indicate that it is possible to incorporate Er into InGaN alloys at the typical growth temperatures of InGaN by optimizing other growth parameters. As confirmed by secondary ion mass spectrometry (SIMS) results shown in Fig. 1(a), we were able to incorporate Er into InGaN with a concentration comparable to that in GaN (as high as $10^{21}$ $cm^{-3}$). It was found that the emission intensity at 1.54 µm decreases with an increase in In-content (Fig. 1(b)).

Table 1. Electrical properties of Er-doped $In_{0.1}Ga_{0.9}N$ epilayers with varying Si co-doping flow rate.

| $In_{0.10}Ga_{0.90}N$: Er+Si | | n ($10^{19}$ $cm^{-3}$) | µ ($cm^2/V$ s) | σ $(\Omega\ cm)^{-1}$ |
|---|---|---|---|---|
| Er (sccm) | Si (sccm) | | | |
| 1 | 0 | N/A | N/A | Too low to be measured |
| 1 | 1 | 0.82 | 86 | 113 |
| 1 | 1.5 | 1.89 | 88 | 270 |
| 1 | 2.5 | 2.94 | 82 | 384 |

It is expected that co-doping will significantly alter the Er dopant's environment. In particular, as shown in Table 1, our results indicate that Si co-doping is necessary to control the electrical conductivity of Er-doped III-nitride epilayers. More work is still needed to fine tune the optimal doping window for achieving high mobility and conductivity.

## B2. Post-Growth thermal annealing process

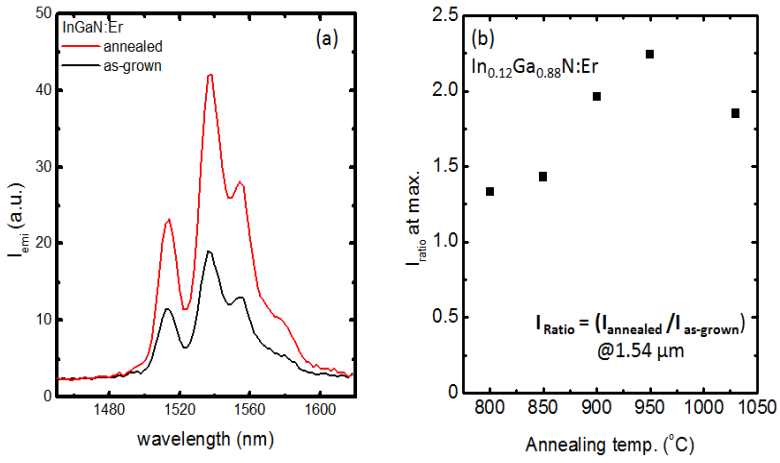


Fig. 2 (a) 1.54 µm emission spectra of as-grown and post-growth annealed Er doped $In_{0.12}Ga_{0.88}N$. (b) Enhancement factor of the 1.54 µm emission intensity from post-growth annealed Er doped $In_{0.12}Ga_{0.88}N$ samples over as-grown Er doped $In_{0.12}Ga_{0.88}N$ measured for varying annealing temperatures. The annealing time is fixed at 1 minute.

Our results shown in Fig. 2 suggest that post-growth annealing improves the Er emission at 1.54 µm. We further evaluated the thermal stability of $In_xGa_{1-x}N$ subjected to post-growth annealing

treatment. We found that InGaN alloys with In concentration below 0.2 are thermally stable [Fig. 3]. This property will allow us to carry out systematic studies on the post-growth thermal annealing dependence by varying the three most important parameters: annealing temperature, time, and gas ambient. This property also ensures that devices based on Er doped $In_xGa_{1-x}N$ with x<0.2 will be thermally stable.

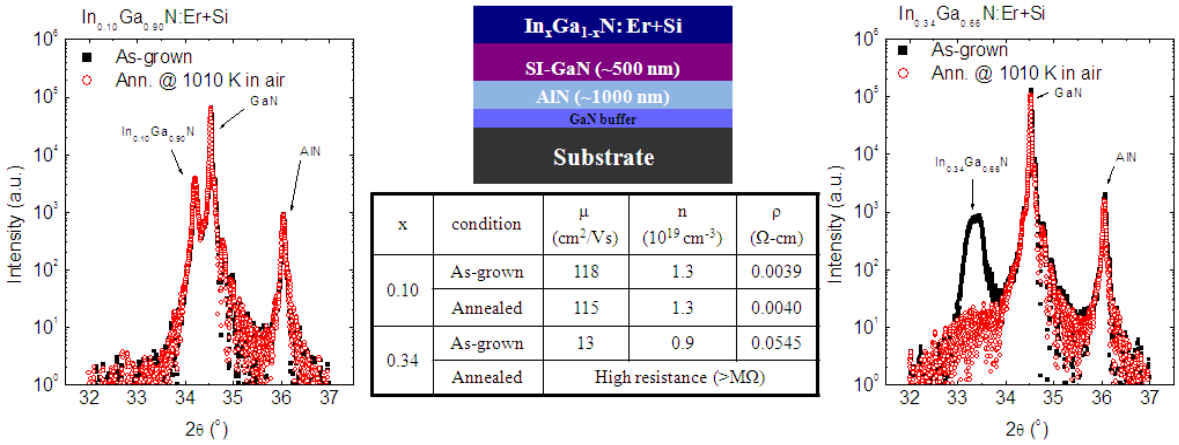


| x | condition | μ ($cm^2$/Vs) | n ($10^{19}$ $cm^{-3}$) | ρ (Ω-cm) |
|---|---|---|---|---|
| 0.10 | As-grown | 118 | 1.3 | 0.0039 |
| | Annealed | 115 | 1.3 | 0.0040 |
| 0.34 | As-grown | 13 | 0.9 | 0.0545 |
| | Annealed | High resistance (>MΩ) | | |

Figure 3 Effects of thermal annealing on the structural (x-ray diffraction spectra of θ-2θ scans) and electrical transport (Hall Effect) properties of Er doped InGaN layers. The XRD peak for $In_{0.34}Ga_{0.66}N$ almost disappear revealing only the electronic properties of the underneath semi-insulating GaN after annealing at 1010 $^0$K in air, whereas the XRD spectral line shape and electron mobility and concentration of $In_{0.10}Ga_{0.90}N$ films remain unchanged after annealing at 1010 $^0$K in air. The results thus indicated that after annealing at 1010 $^0$K in air, $In_{0.34}Ga_{0.66}N$ evaporated, while $In_{0.10}Ga_{0.90}N$ retained the same properties as those of as-grown.

## B3. Growth of Er doped InGaN alloys on Si (001) substrates

In collaboration with Professors N. Sawaki and Y. Honda in Japan, TTU PIs used selective area growth (SAG) and epitaxial lateral overgrowth (ELO) techniques to prepare GaN/AlN/Si(001) templates. As indicated by the schematic in Fig. 4 (a), the periodic lined grooves with the sidewalls of Si (111) and Si $(\bar{1}\,\bar{1}\,1)$ facets were obtained byselectively etching from 7.3$^o$ off-oriented Si (001) substrate by KOH chemical solution, and Si $(\bar{1}\,\bar{1}\,1)$facets were then coated with $SiO_2$ protective films to limit the III-nitride growth only along Si <111> direction. An AlN intermediate layer of 70 nm was first grown on the patterned Si (001) substrate, and followed by the deposition of c-GaN alloy along Si <111> direction until the overgrown layers were merged and the surface became smooth, as shown in the cross-sectional scanning electron microscope (SEM) image, Fig. 4(b). Growth using SAG and ELO techniques not only reduced the difference in thermal expansion coefficient by rotating the direction of c-GaN growth, but also limited the propagation of dislocations. Smooth, crack-free GaN $(1\bar{1}\,01)$ films were formed parallel to Si (001) substrate.

For comparison, GaN/AlN/Si (111) and GaN/AlN/$Al_2O_3$ templates were also prepared by depositing the epitaxial layers directly on respective substrates, as illustrated in Fig. 4(c). θ-2θ XRD spectra measured from these templates are shown in Fig. 5. While GaN (002) peaks were detected at 34.54$^o$ and 34.56$^o$ from GaN/AlN/Si (111) and GaN/AlN/$Al_2O_3$, respectively, the GaN $(1\bar{1}\,01)$ peak at 36.80$^o$ was measured from the GaN/AlN/Si(001). For the GaN/AlN/Si(111) template, the shifted GaN (002) peak from the 2θ diffraction peak of strain-free c-GaN at 34.57$^o$ also implied a stronger compressive stress in c-direction (and tensile stress in a-plane). In contrast, by using ELO growth, the strain of the overgrown semi-polar GaN $(1\bar{1}\,01)$ on the patterned Si (001) substrate was relatively relaxed.

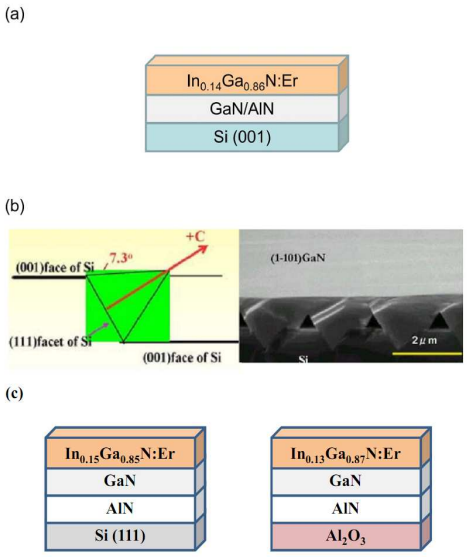


Fig. 4 (a) Schematic of GaN/AlN/Si (001) template, (b) cross-sectional SEM image of a GaN/AlN/Si(001) template obtained by selective area growth and epitaxial lateral overgrowth, and (c) Schematic of the multilayer structures of InGaN alloys grown on Si (111) and $Al_2O_3$ substrates.

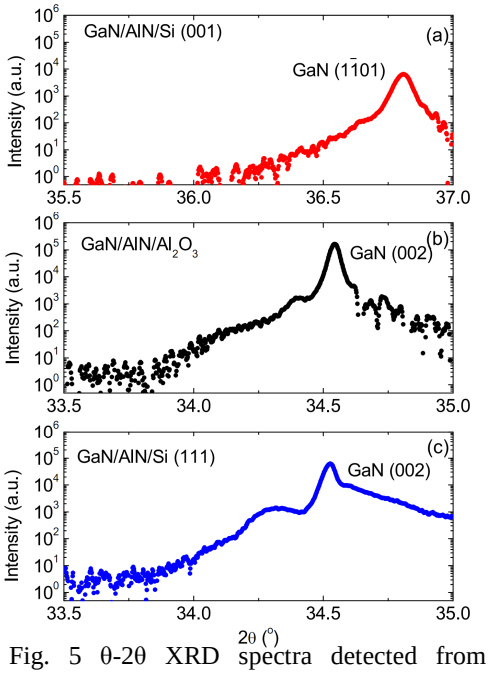


Fig. 5 θ-2θ XRD spectra detected from different templates used for Er doped InGaN growth: (a) GaN/AlN/Si (001), (b) GaN/AlN/$Al_2O_3$, and (c) GaN/AlN/Si(111).

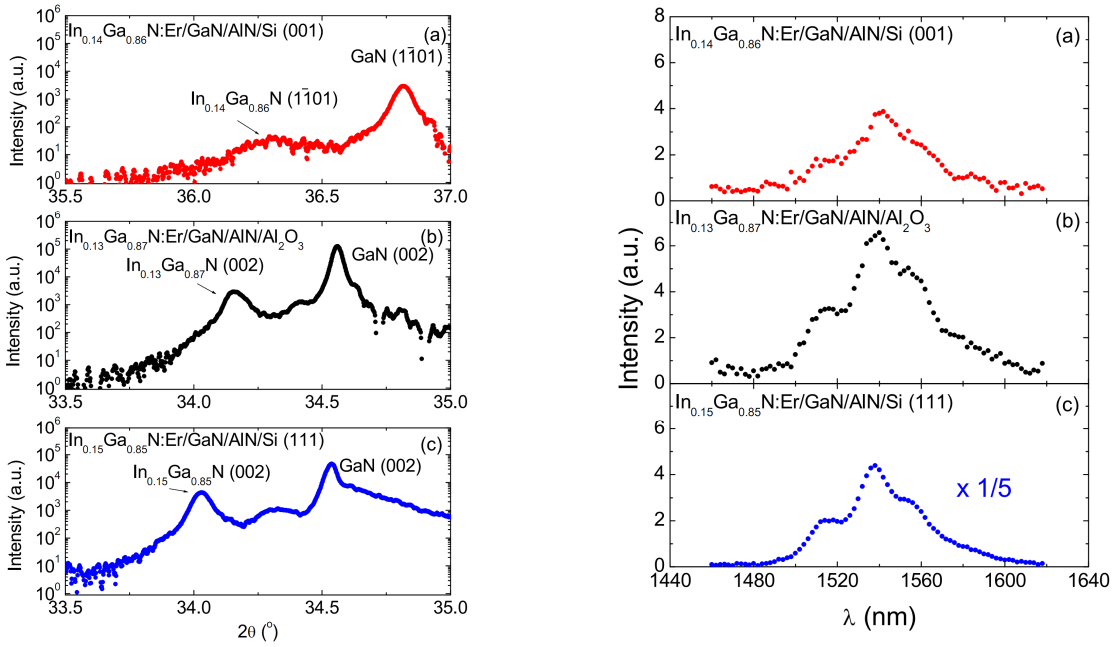


Fig. 6 (Left) θ-2θ XRD spectra and (Right) room temperature infrared PL emission spectra near 1.54 µm measured from $In_xGa_{1-x}N$:Er (x~0.14) grown on different templates: (a) $In_{0.14}Ga_{0.86}N$:Er/GaN/AlN/Si(001), (b) $In_{0.13}Ga_{0.87}N$:Er /GaN/AlN/$Al_2O_3$, and (c) $In_{0.15}Ga_{0.85}N$:Er/GaN/AlN/Si(111).

GaN/AlN/Si(001) templates were employed for the subsequent growth of Er doped InGaN epilayers (InGaN:Er). Figure 6(Left) shows θ-2θ XRD spectra of these InGaN:Er samples. The wurtzite $In_{0.14}Ga_{0.86}N$ $(1\bar{1}01)$ facet was observed from InGaN:Er/GaN/AlN/Si(001) sample with a 2θ peak at 36.29°, while InGaN (002) peaks were detected from InGaN:Er/GaN/AlN/Si(111) and InGaN:Er/GaN/AlN/$Al_2O_3$ samples at 34.04° (In%~15%) and 34.16° (In%~13%), respectively. A small difference in In contents between these three samples could be attributed to the non-uniform strain and In distribution or different growth rates. Under the same growth conditions, the growth of InGaN $(1\bar{1}01)$ facet was found to be two times slower than that of InGaN (0001) facet. Photoluminescence (PL) spectra, focused mainly on 1.54 μm emission, were used to characterize the optical properties of InGaN:Er epilayers grown on various templates. No PL signal was detected in InGaN:Er films grown directly on Si (001) substrate. In contrast, as shown in Fig. 6(Right), 1.54 μm emission was obtained from the InGaN:Er epilayer grown on the GaN/AlN/Si(001) template prepared by SAG. The intensity of 1.54 μm emission obtained from InGaN:Er sample grown on GaN/AlN/Si(001) template was found to be about 1.5 times and 5 times weaker than those grown on GaN/AlN/sapphire and GaN/AlN/Si(111) templates, respectively. The reduced growth rate of InGaN $(1\bar{1}01)$ facet results in a thinner Er-doped InGaN $(1\bar{1}01)$ layer, which attributed in part to the lower intensity of the 1.54 μm emission and XRD signal.

Further improvement of 1.54 μm emission and crystalline properties of Er doped III-nitrides grown on Si (001) substrates is expected in Phase II by optimizing the growth conditions of InGaN:Er $(1\bar{1}01)$ alloys.

**B4 Waveguide amplifier fabrication and carrier lifetime characterization**

Due to the short carrier lifetime in semiconductor optical amplifiers (such as InGaAsP-based devices), cross-saturation causes significant inter-channel crosstalk between different wavelength channels, which is a major problem preventing its applications in WDM systems for signal amplification. In fact, short lifetime is intrinsic to free carriers involved in the band-edge recombination in direct bandgap semiconductors. In order to realize optical amplifiers based on Er doped III-nitrides which potentially possess the advantages of both semiconductor optical amplifiers (small size, electrical pumping, ability for photonic integration) and Er-doped fiber amplifiers (minimal crosstalk between different wavelength channels in WDM optical networks), it is important to characterize the carrier recombination lifetime of the 1.54 μm emission line due to the intra 4*f* shell transition from the excited state ($^4I_{13/2}$) to the ground state ($^4I_{15/2}$) of the Er ions when they are doped in III-nitride semiconductors.

The waveguides were fabricated using optical lithography and inductively coupled plasma (ICP) dry etching. A 250 nm $SiO_2$ passivation layer was deposited on top of the waveguides by plasma enhanced CVD to reduce the optical scattering and loss. The layered structure of the waveguide is shown in Fig. 7(a) with a dimension of 5 μm in width and 2.6 mm in length. The 0.5 μm thick Er-doped GaN layer has an Er concentration of approximately $5\times10^{20}$ $cm^{-3}$.

To evaluate the carrier lifetime, a 1480 nm pump laser was used as an excitation source and the spontaneous emission signal was collected through a bandpass optical filter at 1537 nm (with 1 nm resolution); An InGaAs photodiode was used to detect the optical power and the waveforms were recorded. By suddenly switching off the 1480 nm pump laser, the decay rate of the photoluminescence at 1537 nm is determined by the carrier lifetime on the excited state (or the $^4I_{13/2}$ energy level). The measured decay kinetics of the spontaneous emission after switching off the pump shown in Fig. 7(b) exhibits a fast time constant of 1.5 ms and a slower time constant of 2.8 ms. The non-exponential decay indicated the existence of Auger recombination and cooperative upconversion which is responsible to excite carriers to higher energy levels. This lifetime is 6 orders of magnitude

larger than those in InGaAsP optical amplifiers and is comparable to those in Er doped optical fibers. This verification of long carrier lifetime confirms the potential of our proposed Er doped III-nitride technology for high speed optical communication applications.

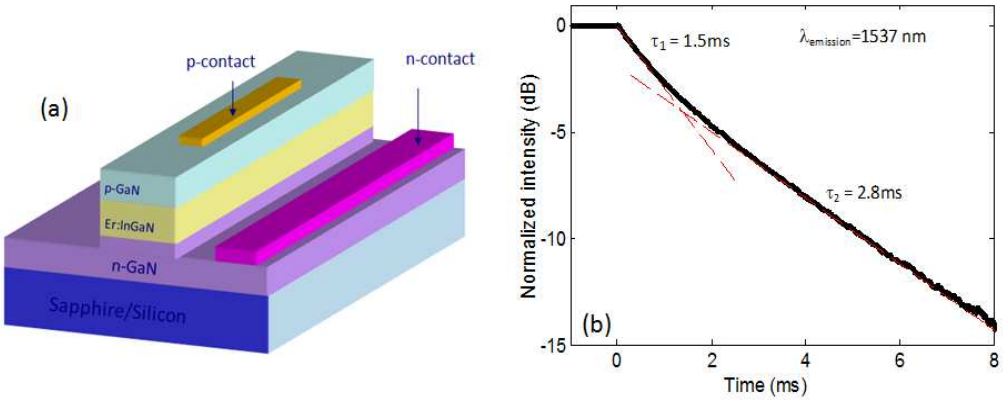


Figure 7(a) Schematic structure of the Er-doped GaN waveguide. (b) The decay of the spontaneous emission at 1537 nm wavelength after the 1480 nm pump laser was switched off at $t = 0$.

## B5. Characterization of refractive indices of Er doped GaN in IR region

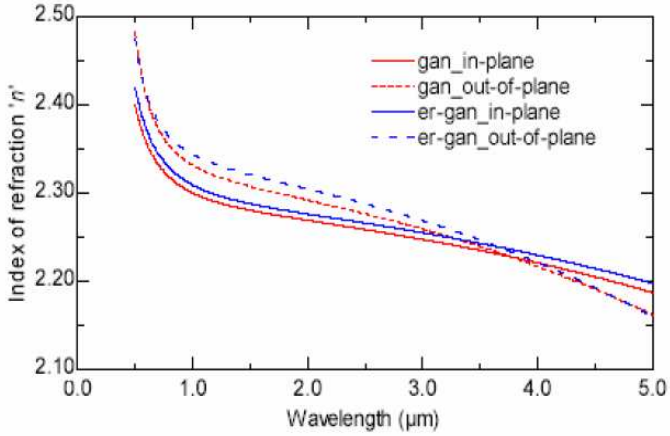


Figure 8 Effects of Er incorporation on the refraction index of GaN measured in the IR wavelength region.

We have investigated the effects of Er doping on the refractive index of GaN. To evaluate the refractive index, optical transmission spectra were measured. Due to the Fabry–Perot (FP) interference caused by the two facets of the film (one facet is between GaN and the air and the other facet is formed between GaN and substrate), optical transmission efficiency is wavelength-dependent. With the knowledge of the film thickness, the film refractive index can be obtained by best fitting the measured optical transmission spectrum to a well-known FP transmission equation. Figure 9 shows the effect of Er incorporation on the refractive index of GaN. The results indicated that the overall increase of refractive index due to Er incorporation is estimated to be around 0.01 at 1.5 μm. Similarly, the estimated refractive index increase due to the incorporation of In (5%) is around 0.015 at 1.5 μm. Knowledge of material refractive index in the operating wavelength region will be important for the optimization of device design.